Numerical Analysis and Performance Optimum of an HTS Suspension Propulsion System Driven by a SLIM

Luhai Zheng, and Jianxun Jin
School of Automation, University of Electronic Science and Technology of China
2006 Xiyuan Road, Gaoxin Western District, Chengdu, Sichuan, 611731, China
Wei Xu, Youguang Guo, and Jianguo Zhu
Faculty of Engineering and Information Technology, University of Technology Sydney
Sydney, NSW 2007, Australia
jxjin@uestc.edu.cn

Abstract — A high temperature superconducting (HTS) magnetic suspension propulsion system driven by a long-primary single-sided linear induction motor (SLIM) has been developed. Equivalent current sheet method is applied to calculate the flux density distribution of the PMG, and it is verified to be accurate by measurements. The levitation force and guidance force of the magnetic suspension sub-system are also calculated by a numerical method. The normal attractive force of the SLIM is undesirable for the magnetic suspension system for which reduces the load capacity. The slip optimum design is carried out in this paper to decrease the normal force with results of a minimize ratio of the normal force to the thrust force and satisfy the thrust force requirements simultaneously.

I. INTRODUCTION

Various kinds of high temperature superconducting (HTS) suspension propulsion systems driven by linear motors have been developed. The developed HTS suspension systems have the types of electro-dynamic (repulsion) suspension (EDS) using HTS coil magnets [1], electro-magnetic (attraction) suspension (EMS) using HTS coils [2], and the HTS magnetic (repulsion) suspension using field-cooling HTS bulks [3].

HTS magnetic suspension system has simple structure, consisting of HTS bulks on the moving low temperature vessels and PM guideway (PMG) on the track. Moreover, it has self-levitation and self-guidance capabilities without any guidance control system. So HTS magnetic suspension system has many advantages when used into maglev and magnetic suspension launching system. The levitation force and guidance force are important performance parameters for the HTS magnetic suspension system. While the guidance force F_{Gui} depends on the trapped flux in the HTS bulk, the levitation force F_{Lev} is linear with the gradient of the magnetic field of PMG. So it is important to design a PMG with high magnetic field gradient.

In this work, an HTS magnetic suspension propulsion system driven by a long-primary single-sided linear induction motor (SLIM) has been developed. Two types of PMGs have been designed for the magnetic suspension sub-system. The equivalent current sheet method is used to build up the PMG numerical model to analyze the flux density distribution, which is the basis for calculating the levitation force and guidance force between the HTS bulk and PMG. The slip (s) optimum design is also carried out to decrease the normal force F_{n} of the SLIM to increase the load capacity of the magnetic suspension propulsion system.

II. MODEL OF HTS MAGNETIC SUSPENSION PROPULSION SYSTEM

The HTS magnetic suspension propulsion system is developed with the model as shown in Fig. 1, which is driven by a long-primary SLIM in the middle and levitated by HTS magnetic suspension sub-systems on both sides of the SLIM. The primary stator of the SLIM consists of iron-core and three-phase concentrated windings, and the secondary is a compound structure which is composed of an Al plate and a back iron (Fe) plate, respectively. Two types of PMG are designed and fabricated with the schematic diagram as shown in Fig. 2, where the arrow direction is the magnetization direction of PM.

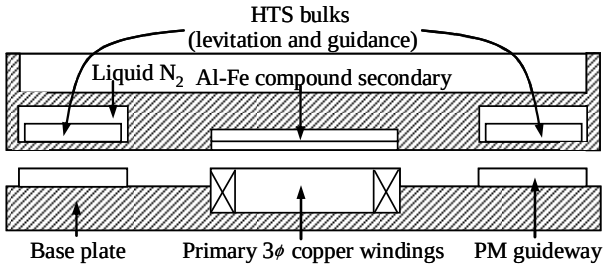

Fig. 1. Model of HTS suspension propulsion system driven by a SLIM.

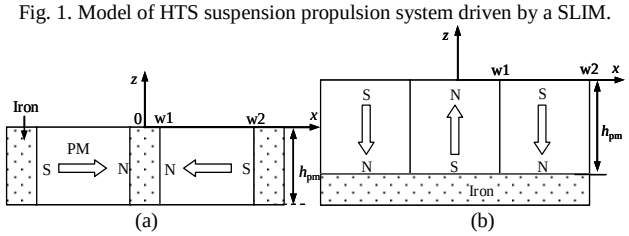

Fig. 2. Structure schematic diagram of the PMG, (a) horizontal array PMG (#1), (b) vertical array PMG (#2).

III. LEVITATION FORCE AND GUIDANCE FORCE

A. PMG Numerical Model

Equivalent current sheet method is used to build the horizontal array PMG and vertical array PMG by ignoring the influences of soft iron on the flux density distribution with the models as shown in Fig. 3(a) and Fig. 3(b), respectively. We can firstly calculate the magnetic field distributions at point (x, z) generated by each current sheet, and then sum all the components.

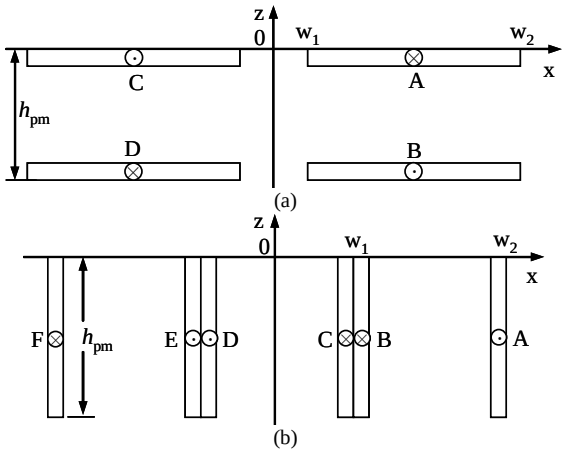

Fig. 3. Current sheet models, (a) horizontal array PMG (#1), (b) vertical array PMG (#2).

Fig. 4 shows the transversal distributions of B_z and B_x at the height h = 1 mm from upper surface of the two PMGs. We can see that the results calculated by numerical method are consistent with those got by measurment, which proves the accuracy of the numerical model built by equivalent current sheet method.

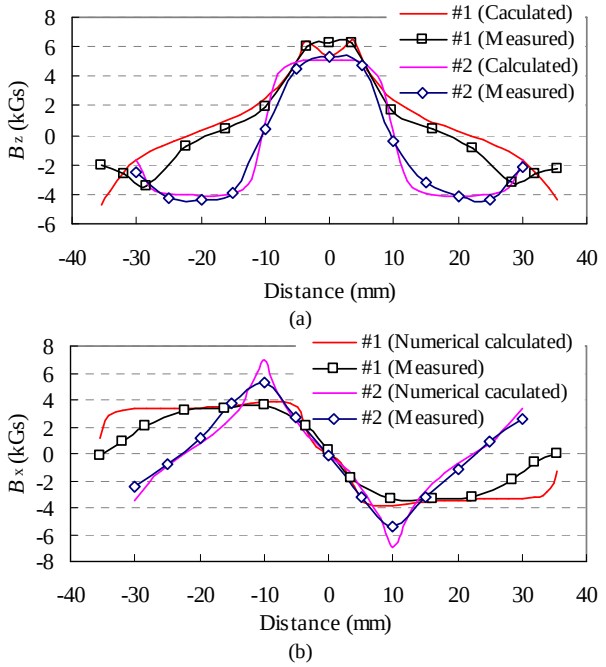

Fig. 4. Distribution of B_z and B_x along transversal direction, (a) B_z, (b) B_x.

B. Levitation Force and Guidance Force

Base on the magnetic field distributions, we can calculate the F_{Lev} and F_{Gui} by

$$F_{Lev} = \int_0^{TH}\int_{L/2}^{L/2-\delta}\int_{W/2}^{W/2-\delta} J_c \times B_x \mathrm{d}x\mathrm{d}y\mathrm{d}z \qquad (1)$$

$$F_{Gui} = \int_0^{TH}\int_{L/2}^{L/2-\delta}\int_{W/2}^{W/2-\delta} J_c \times B_z \mathrm{d}x\mathrm{d}y\mathrm{d}z \qquad (2)$$

where TH, L, W are the thickness, length and width of HTS bulk, δ is the depth of field penetration, and $\delta = (B_z - B_{zfc})/\lambda\mu_0 J_c$, where B_{zfc} is the trapped magnetic field of HTS bulk, λ the Nagaoka coefficient determined by the configuration of a sample, J_c the critical current density, μ_0 the permeability of vacuum.

IV. SLIP OPTIMUM OF SLIM AND CONCLUSIONS

Using the equations of $P_o = F_x \cdot v_r$ and $s = (v_s - v_r)/v_s$ electromagnetic thrust F_x of the SLIM can be calculated as

$$F_x = \frac{P_o}{v_r} = \frac{3I_2^2R_2}{sv_s} = \frac{3sI_1^2R_2G^2}{v_s\left[(sG)^2+1\right]} = \frac{3(v_s-v_r)I_1^2R_2G^2}{(v_s-v_r)^2G^2+v_s^2} \qquad (3)$$

The final expression of normal force F_n is

$$F_n = -\frac{W_{se}p\tau^3}{\pi^2}\frac{\mu_0 J_m^{\,2}}{g_e^{\,2}(1+s^2G^2)}\left[1-\left(\frac{\pi}{\tau}g_e sG\right)^2\right] \qquad (4)$$

All above variables are used as their conventional meanings as defined in [4]. In the low speed region, the normal force is attractive force (negative), but for high speeds, it may become repulsive (positive). From (4) the condition in which the repulsive force component dominates is

$$1-\left(\frac{\pi}{\tau}g_e sG\right)^2 < 0 \Rightarrow s > s_t = \frac{\rho_s}{2\mu_0 f\tau} = \frac{1}{\sigma_s\mu_0 v_s} = \frac{1}{R_m} \qquad (5)$$

where $R_m = \sigma_s\mu_0 v_s$ is the magnetic Reynolds number, σ_s the face electrical conductivity of Al. When s_t = 1, based on the parameters of SLIM we can obtain the critical frequency f_c = 33.354 Hz, which tells that only when f > 33.354 Hz, it exists an s to make the normal force be a repulsive force or a value equal to zero. The repulsive levitation force is available at a cost in the motor dissipative losses, and hence its feasibility would depend on tradeoff against costs of aircushion and other methods. The relationship between the normal force and the thrust force can be studied from the ratio

$$\frac{F_n}{F_x} = \frac{k_w}{2}\left(R_m s - \frac{1}{sR_m}\right) \qquad (6)$$

where k_w is the winding factor. This ratio is useful for the design purposes especially when the thrust force is normalized with respect to the weight of the vehicle.

V. REFERENCES

[1] C. Y. Lee, J. M. J. M. Jo, Y. J. Han, D. K. Bae, Y. S. Yoon, S. Choi, *et al.*, "Estimation of current decay performance of HTS electromagnet for maglev," *IEEE Trans. Appl. Supercond.*, vol. 20, no. 3, pp. 907-910, 2010.

[2] S. Kusada, M. Igarashi, K. Nemoto, T. Okutomi, S. Hirano, K. Kuwano, *et al.*, "The project overview of the HTS magnet for superconducting maglev," *IEEE Trans. Appl. Supercond.*, vol. 17, no. 2, pp. 2111-2116, 2007.

[3] J. S.Wang, S. Y.Wang, Y. Zeng, H. Y. Huang, F. Luo, Z. P. Xu, *et al.*, "The first man-loading high temperature superconducting maglev test vehicle in the world," *Physica C*, vol. 378–381, pp. 809-814, 2002.

[4] L. H. Zheng, J. X. Jin, Y. G. Guo and J. G. Zhu, "Design and characteristics analysis of long-primary single-sided linear induction motor," *2009 IEEE International Conference on Applied Superconductivity and Electromagnetic Devices*, 25-27 September 2009, pp. 85-88, Chengdu, China.